Lead equivalence testing using a custom-built testing kit.

Lesley Maddox (Lesley.Maddox@health.wa.gov.au)
Sir Charles Gairdner Hospital https://orcid.org/0000-0003-2734-9280
Robert Parin
Sir Charles Gairdner Hospital
Benjamin Khoo
Sir Charles Gairdner Hospital

Research Article

Keywords: Radiation protective garments, lead equivalence testing, broad beam geometry, filtration, custom-built testing kit

Posted Date: June 23rd, 2022

DOI: https://doi.org/10.21203/rs.3.rs-1763806/v1

Abstract

Radiation protective garments should undergo a quality assurance regime comprising of an acceptance test of the lead equivalence before the garment is introduced into clinical service, followed by routine periodic visual and fluoroscopic inspections throughout its remaining clinical lifespan. The IEC 61331-1:2014[1] is the leading standard outlining the methodology for testing of lead equivalence of these garments and forms the basis of the Australian/New Zealand Standards(1999)[2]. This study outlines the design and development of an IEC compliant broad beam lead equivalence testing setup, using an in-house custom-built testing kit (CBTK). The practicality and robustness of this kit was performance tested using lead equivalence measurements on 97% pure lead sheets. Hospital radiation protective garments are predominantly made of lead-free or lead-composite materials due to their light weight, as such, a set of lead-free (N-Pb) samples was also performance tested. These samples were tested using two different beam qualities; a total filtration of 2.5 mmAl and 0.25 mmCu added filtration, both at 102 kVp. Samples with thicknesses of 0.25 mm, 0.35 mm and 0.50 mm were used. The differential between labelled and measured lead equivalence averaged 3% for both the 'pure-lead' samples and N-Pb samples, with uncertainty of less than 7%. At 102 kVp, the use of Cu or Al filtration has marginal effect on measured lead equivalence for pure lead or N-Pb samples. The efficacy of utilizing the CBTK with a solid-state detector for lead equivalence testing was demonstrated through its ease of use, consistency and precision.

Introduction

Radiation protection, radiation safety and quality assurance are important and integral components of a Diagnostic Imaging Medical Physicists' (DIMP) responsibilities. To that end, testing and screening of lead, lead-composite, or lead-free radiation protection garments for their xray attenuation or radiation shielding efficacy is imperative to ensure adequate radiation protection is provided to staff. Quality assurance (QA) of radiation protective garments, or more importantly, lead equivalence testing is provided in Standards and guidelines, i.e. Australian/New Zealand Standards (AS/NZS) (1999)[2], IEC (2014, 1994)[1,3], and Australian Radiation Protection and Nuclear Safety Agency (ARPANSA)[4]. The AS/NZS (1999)[2] make reference to an outdated version of the IEC standards (IEC (1994)[3], which has since been superseded in 2014 (IEC (2014))[1].

Neither the IEC (2014, 1994)[1, 3] or the AS/NZS (1999)[2] explicitly state which geometry or beam configuration should be used for the testing of lead equivalence, suggesting that either broad beam geometry or narrow beam geometry is acceptable. Furthermore, the type and amount of material used as beam filtration (i.e. beam quality) was changed from 0.25 mmCu added filtration in the old IEC (1994)[3] standard to 2.5 mmAl total filtration in the new IEC (2014)[1] standard.

This presents a challenging task for physicists in Australia and New Zealand who are bound from a legislative perspective to follow the old recommendations of AS/NZS (1999)[2] until existing standards and guidelines are updated.

In this study, we present the development of a custom-built testing kit (CBTK) based on broad beam geometry which complies with both AS/NZS (1999)[2] and IEC (2014)[1]. By simply changing the amount of added filtration from 0.25 mmCu to 2.5 mmAl, the setup can be used to test under the guidelines of either the old standard[3] or new standard[1]. The setup was performance tested by verifying the measured lead equivalent thickness against a set of 97% 'pure lead' sheets (with 1.5% Sn and 1.5% Sb impurities) of discrete and known thicknesses.

Given that it is now more common to find radiation protective garments made from lead-free or lead-composite materials[5], it was considered relevant to test the efficacy of the CBTK and setup with these sample types. In Australia, the minimum attenuation equivalent for light radiation protective garments is 0.25 mm Pb and for heavier radiation workloads such as those in cardiac, vascular or neuro-interventional procedures, the minimum requirement is 0.35 mm Pb[6]. Thyroid collars are typically 0.50 mm Pb. Thus, three lead-free (N-Pb) samples of varying thickness (0.25, 0.35 and 0.50 mm) were also tested and compared using the two different beam qualities. No lead-composite samples were used in this study.

The aim of this study was firstly, to design and develop the CBTK for lead equivalence testing. Secondly, having established a consistent and robust setup, the CBTK was used to performance test 97% pure lead samples of various thicknesses. Thirdly, lead equivalence testing of samples from N-Pb materials were tested using the CBTK in the same set-up. Lastly, since N-Pb materials are known to vary under different beam qualities[7], the kit was used to investigate the effects of Cu and Al as added filtration materials, on the measured lead equivalence.

Materials And Methods

IEC 61331.1:2014 broad beam conditions

To minimise the introduction of errors during setup and following the requirements of the IEC (2014)[1] standards, a CBTK for lead equivalence testing was designed and engineered by co-author, Robert Parin (RP) so that each setup would remain stable, consistent and reproducible. A diagram detailing the linear dimensions of various components of the CBTK within the broad beam setup is provided in Fig. 1, with the corresponding schematic shown in Fig. 2.

The use of the CBTK ensures that when the x-ray tube focal spot is positioned 1.55 m from the floor, all other distances relative to the focal spot will be consistently maintained, as per Fig. 1. The broad beam geometry, as defined by IEC (2014)[1] has two essential conditions that need to be fulfilled. The first condition (Eq. 1) is the distance between the x-ray tube focal spot and the bottom of the sample, denoted '*a*', must be at least equal to three times the diameter of the beam shaping lead diaphragm '*d*' closest to the detector IEC (2014)[1].

$a \geq 3d$ (Eq. 1)

The setup in Fig. 1 shows that distance '*a*' is approximately 15 times greater than *'d'*. The second condition (Eq. 2) requires the diameter of the lower diaphragm '*d*' to be greater than or equal to 10 times the distance between the sample and the sensitive area of the radiation detector '*b*' IEC (2014)[1], based on the geometry in Fig. 1, *'d'* is exactly equal to *10b*.

$d \geq 10b$ (Eq. 2)

Thus, with the CBTK utilized in the configuration outlined in Fig. 1, the two essential IEC (2014)[1] conditions will always be met.

Custom-built testing kit (CBTK)

Model consideration

ARPANSA published a lead equivalence testing setup in 2015[4]. This setup however, does not conform to either the broad beam or narrow beam geometry as defined by IEC (2014)[1], mainly due to the location of the sample relative to

the beam shaping lead diaphragm. Furthermore, where the IEC (2014)[1] specifies the use of two beam shaping lead diaphragms (Figure 1), ARPANSA (2015) [4] and the AS/NZS[2], only specify the use of one.

In this study, we adopted the use of broad beam geometry to reflect and reproduce the scenario in which a radiation protective garment is exposed to clinically. A broad beam is the most analogous model to fit the broadly scattered radiation arising from a patient. The CBTK (Figure 2) was designed and fabricated by co-author RP to incorporate the dimensions of the two beam shaping lead diaphragms according to the IEC (2014)[1] broad beam setup (Figure 1). The 1.55 m x-ray tube focal spot to floor distance, the 0.2 m between the beam shaping lead diaphragm and the sample were retained from ARPANSA[4].

The schematic of the CBTK (Figure 2) shows the two beam shaping lead diaphragms (A and B), both comprising of 4.5 mm of lead supported between two thin sheets of Perspex.

In the Figure 1 setup, the x-ray tube must be positioned 1.55 m from the floor with the diaphragms aligned centrally to the crosshairs of the x-ray tube light field. As per the dimensions, the two beam shaping lead diaphragms within the CBTK collimate the x-ray field to a 10 x 10 cm square at the entrance surface of the sample. The lower lead diaphragm (B) serves a threefold purpose as an attenuator, collimator and platform. In theory, its position below diaphragm (A) is designed to absorb scattered radiation originating in the air gap between the two diaphragms as well as scatter from the sample. With scattered radiation sufficiently attenuated by the lead, the beam is finally collimated to fulfil the broad beam conditions. Practically, the lower diaphragm also serves as a platform on which the samples can be placed. Plastic legs support the CBTK on the floor and steadily suspend the lead diaphragms at their fixed positions whilst allowing ample room for full-sized radiation protective garments to be unfolded and manoeuvred on top of the diaphragm B platform. An in-built cradle is used to consistently position the radiation detector at the correct location and orientation for each test, i.e. elevating the radiation detector from the ground and maintaining the precise distance to the sample to satisfy broad beam conditions[1].

Filtration and beam quality

Part 1 of the AS/NZS[2] provides a table outlining the amount of added filtration (mmCu) that should be used for each corresponding tube voltage, for example, at 100 kVp, the recommended amount of added filtration is 0.25 mmCu. Conversely, the current IEC (2014)[1] standard states that a total filtration of 2.5 mmAl should be used for all tube voltages. In this study, dose measurements were taken with a solid-state radiation detector to determine the lead equivalent thickness of a set of ‘pure-lead’ samples and a set of N-Pb samples. Each set of samples (‘pure-lead’ or N-Pb) were tested twice at 102 kVp, first using 0.25 mmCu added filtration and again with 2.5 mmAl total filtration. The decision to test the samples at 100 kVp was based on the stated tube voltage guaranteed on the label of the N-Pb sample material. The nearest increment to 100 kVp that the radiographic x-ray unit was able to achieve was 102 kVp.

Calibration

All lead equivalence measurements in this report were made using a Philips Optimus 80 (*SN:10000170*) fixed radiographic x-ray unit located in the Department of Radiology at Sir Charles Gairdner Hospital (SCGH), Western Australia. This unit was compliant for clinical use as required by the Radiological Council of Western Australia[8] at the time the measurements were taken. Attenuation measurements were made using a calibrated RTI Piranha 657 Internal Probe solid-state detector (*SN:CB214120963*).

A two-fold calibration and verification process were performed. High purity 99.95% pure lead sheets of 0.1 mm thickness and 15 x 15 cm^2 in size (Goodfellow Cambridge Ltd, England, UK), were used for the calibration. Three measurements were made without attenuation to obtain the unattenuated intensity, I_0 (Eq. 3). This was followed by attenuation measurements using the above-mentioned high purity lead sheets. Starting the attenuation with 0.1 mm Pb, and increasing the thickness in increments of 0.1 mm, to a maximum thickness of 0.6 mm Pb. Three measurements were taken at each increment. This enables the beam quality of the x-ray beam spectrum to be determined (Equations 3 and 4), where I is the attenuated intensity, μ is the linear attenuation coefficient, x is the thickness of attenuator (0.1, 0.2, 0.3, 0.4, 0.5, 0.6 mm Pb), and HVL the half-value layer.

$I = I_0 e^{-\mu x}$ (Eq. 3)

$HVL = \frac{\ln(2)}{\mu}$ (Eq. 4)

Air kerma measurements taken through samples are thus converted into a 'measured thickness' via Eq. 3, and then corrected by applying them through the equation for the second order polynomial regression line in the calibration curve. By utilizing a calibration curve obtained from pure lead sheets, the corrected value represents the lead equivalent thickness of the sample materials expressed in mm Pb.

Verification using 'pure-lead' samples

A second set of lead sheets (Goodfellow Cambridge Ltd, England, UK), composed of 97% Pb, 1.5% Sn (Tin) and 1.5% Sb (Antimony) were used to verify the measured lead equivalence with the true thickness of the samples within a reasonable margin of error. Each verification sample was 0.05 mm thick and 15 x 15 cm^2 in dimensions. When appropriately stacked together, these sheets can be assembled to reproduce the typical clinical thicknesses found in radiation protection garments (i.e. 0.25, 0.35 and 0.50 mm Pb).

Lead-free (N-Pb) samples

Following the verification tests on the 'pure lead' samples, the measured lead equivalence of the N-Pb samples were then evaluated. The N-Pb samples used were from clinically available 'aprons' from a single radiation protective garment manufacturer. As with the 'pure lead' samples, three sample thicknesses of the N-Pb materials were obtained (0.25 mm, 0.35 mm and 0.50 mm) for comparison. The 0.50mm sample was comprised of a double layer of the 0.25mm material. Preliminary fluoroscopic screening tests on all samples prior to the lead equivalence measurements confirmed that the internal protective material was uniform and intact. The N-Pb samples were stated by the manufacturer to be composed of a bilayer containing Antimony (Sb) and Tungsten (W). It is assumed that any rubber or polymers bonded to the material to provide the garment its flexibility are not contaminated with any other heavy metals that would affect its attenuation characteristics. The bilayer arrangement of the non-lead samples used in this study have a lower atomic number (Sb, Z=51) as the first layer and a higher atomic number as the second layer (W, Z=74). The first layer being the initial layer that the incident x-rays encounter in the bilayer configuration. In theory, k-edge fluorescent x-rays created within this first layer are absorbed in the second layer. The directionality of the samples when placed on the CBTK is thus crucial when bilayer materials are tested, i.e. to ensure the correct side is facing the incident x-ray beam. The manufacturer stated energy rating of the N-Pb samples was labelled 100 kVp and thus all tests in this paper were conducted at the closest available tube voltage of 102 kVp.

Results

Measurement uncertainty was less than ± 0.02 mm Pb for all (pure lead and lead-free) 0.25 and 0.35 mm Pb samples and ± 0.03 mm Pb for all 0.50 mm Pb samples tested. The relative standard uncertainty (%) in Table 1 is derived from the standard deviation of the mean values for each parameter across repeated calibration measurements using the same x-ray technique factors.

Table 1
Type A and B relative standard uncertainties (%).

Source of Uncertainty	Type A	Type B
Linear attenuation coefficient (μ)	4.0	-
Calibration curve	2.4	-
Measured air kerma	1.0	-
Radiation detector (Piranha base unit)	-	5.0
	4.8	5.0
Total	6.9	

It is assumed that the N-Pb samples are labelled with a lead equivalent thickness that is accurate to within a reasonable margin of error. IEC (2014)[1] states a relative standard uncertainty of 7% should be considered in the decision of conformity to the labelled value. This uncertainty is unfortunately caveated under inverse broad beam geometry conditions and therefore cannot be assumed to apply to broad or narrow beam geometry. At SCGH, a conservative rejection criterion of 10% has been adopted.

Figure 3 shows results from testing the 'pure lead' verification samples under 0.25 mmCu filtration. The calibration corrected measurements show strong agreement to the line of unity. The differential between the measured and true thickness averaged 2.8% for tests performed under Cu and Al filtration (Tables 2 and 3).

Table 2
Results of lead equivalence tests using exposure factors 102 kVp, 50 mAs, 63.7 ms with 0.25 mmCu added filtration.

Samples	Material composition	Label (mmPb)	Average measured (mmPb)	Uncertainty ± (mmPb)	Percentage Difference* (%)	Transmission† (%)	Attenuation‡ (%)
Pb verification samples	Pb (97%), Sn (1.5%), Sb (1.5%)	0.25	0.26	0.02	2.9	21.9	78.1
		0.35	0.36	0.02	2.6	14.2	85.8
		0.50	0.52	0.03	3.0	7.9	92.1
Non-lead samples	Sb + W	0.25	0.25	0.02	-1.6	23.1	76.9
		0.35	0.36	0.02	1.7	14.4	85.6
		0.50	0.52	0.03	3.7	7.8	92.2

* Percentage difference = (measured – labelled)/labelled * 100

† Transmission = $(I/I_0)*100$; ‡ Attenuation = (1-Transmission)

Table 3
Results of lead equivalence tests using exposure factors 102 kVp, 50 mAs, 63.7 ms with 2.5 mmAl total filtration.

Samples	Material composition	Label (mmPb)	Average measured (mmPb)	Uncertainty ± (mmPb)	Percentage Difference* (%)	Transmission† (%)	Attenuation‡ (%)
Pb verification samples	Pb (97%), Sn (1.5%), Sb (1.5%)	0.25	0.26	0.02	3.3	13.7	86.3
		0.35	0.36	0.02	2.8	8.6	91.4
		0.50	0.51	0.03	2.4	4.6	95.4
Non-lead samples	Sb + W	0.25	0.23	0.02	-6.4	15.5	84.5
		0.35	0.34	0.02	-1.7	9.2	90.8
		0.50	0.52	0.03	3.4	4.6	95.4

* Percentage difference = (measured – labelled)/labelled * 100

† Transmission = $(I/I_0)*100$; ‡ Attenuation = (1-Transmission)

Tables 2 and 3 present the measurement outcomes based on exposure factors 102 kVp, 50 mAs and 63.7 ms for Cu and Al filtration respectively. The results from testing the verification samples showed agreement to within 3.0% of the actual thickness using the Cu filtration and less than 3.3% using Al filtration (Tables 2 and 3), demonstrating a tendency to be marginally overestimated under both types of filtration. The similarity in magnitude of the results under both Cu and Al suggests that measured lead equivalence of the verification samples is unaffected by differences in filtration.

The measured lead equivalence of the N-Pb samples was variable. Under Cu filtration, the 0.25 mm and 0.35 mm N-Pb samples resulted in a lower percentage deviation from their labelled value than the verification samples. The differential from labelled value was at most 1.7%, lower than observed from the verification samples (3.0%). The exception was with the 0.50 mm thickness, where the N-Pb sample behaved relatively similar to the verification sample.

The same was not true under Al filtration. All three N-Pb samples tested under Al filtration resulted in a lower measured lead equivalence than when measured under the Cu filtration. The 0.25 mm sample was underestimated (-6.4%) compared to the labelled value as was the 0.35 mm sample but to a lesser extent (1.7%). The 0.50 mm N-Pb sample was the least affected by the change in filtration and resulted in a greater measured lead equivalence than the 0.50 mm verification sample under both Al and Cu.

Discussion

The measured outcomes from the verification samples were marginally higher than their true thickness (Figure 3). This may be due to the presence of the elemental ‘impurities’ (Sn and Sb) which enhance the attenuation properties of the verification samples due to their k-edge spectra. While the presence of impurities had a positive impact on the performance of the verification samples, the differential was insignificant, to around 3.0% (Tables 2, 3) and shows a good fit to the line of unity (Figure 3).

The N-Pb samples are composed of antimony (Sb) and tungsten (W). W has a k-edge at 69.5 keV, an l-edge at 10.2 keV and Pb has a k-edge at 88 keV (Figure 5). Between effective energy range of 69 keV and 88 keV, attenuation of these combined materials’ (Sb and W) will be significantly better compared to pure Pb. However, the converse is true for effective energies greater than 88 keV. The attenuation differential between Pb and N-Pb materials will be more

pronounced for thinner as opposed to thicker samples. In the effective energy range of less than 69 keV, the mass attenuation coefficients of both Pb and N-Pb materials are declining at a similar magnitude (Figure 5). Thus, for corresponding thicknesses, the attenuation for the Pb and N-Pb samples below 69 keV will be marginally different, as seen in the results (Tables 2 and 3).

Figure 4 comparatively shows the simulated bremsstrahlung spectra through 2.5 mmAl as opposed to 0.25 mmCu. The Al filtered bremsstrahlung spectra is shown to remove a small portion of low energy x-rays up to 12 keV, after which the spectra begins to rise, peaking at 42 keV. In comparison, the relative number of photons from the Cu filtered spectra over the same energy range is much lower. Cu is highly efficient at attenuating photons below 22 keV and thus the peak intensity of photons occurs at a higher energy (51 keV) compared to Al (42 keV). The large differential between the two spectra clearly demonstrates that a significant proportion of low energy x-rays are removed from the x-ray spectra due to the Cu filtration alone, i.e. the Cu spectra produces a more penetrating beam.

In comparison to Cu, Al filtration produces a less penetrating beam which also means there is a higher proportion of x-ray photons in the spectra (Figure 4). With more x-ray photons incident on the sample and a lower effective energy compared to a Cu filtered spectra, there is a potential for higher attenuation under Al filtration. The 0.25-, 0.35- and 0.50-mm Pb verification and N-Pb samples showed similar 9%, 6% and 3% respectively more attenuation under Al filtration compared to Cu filtration (Tables 2 and 3).

The effectiveness of the bilayer can be explained as follows; the initial layer of Sb effectively attenuates incident photons between 30.5-60 keV due to its k-edge at 30.5 keV (Figure 7). Transmitted x-rays as well as any fluorescent x-rays emitted in the initial Sb layer are then filtered through the W layer. This directional bilayer effect impacts the manner in which samples are placed during testing. The 0.50 mm non-lead sample is comprised of two 0.25 mm bilayer sheets.

There are two fundamental characteristics to a bremsstrahlung spectrum. The first being the inverse linear relationship between the number of photons and the photon energy. Secondly, a filtered bremsstrahlung spectrum (Figure 4) will have an effective energy between one-third to one-half of the maximum tube potential[10]. This effective energy is determined by filtration of the x-ray beam and the maximum tube potential (kVp). It thus follows that attenuation is optimised when the material k-edge is aligned with the effective energy of the bremsstrahlung spectrum. If the x-ray beam effective energy is too far from the material's k-edge, attenuation will decrease accordingly, thus the energy dependence of lead equivalent testing. It is suggested that this variation can be up to 20% and pure-lead samples are not affected[11].

It is thus acknowledged that testing at a single energy (102 kVp) can perpetuate biased results as it gives an incomplete characterisation of a N-Pb garment's attenuation properties[12]. However, while testing lead equivalence at a single energy is considered a non-desirable practice [12], it is a pragmatic and practical approach for busy medical physics departments. Further, it is customary to find radiation protective garment labels which guarantee their product at only one specific tube voltage (kVp). The N-Pb samples used in this study were specified for their lead equivalence exclusively at 100 kVp.

Limitations of this study

The Piranha 657 Internal Probe is a new generation QA dosimeter commonly found and used in hospital based medical physics departments throughout Australia, due to its reliability, versatility and ease of use. The motivation to use the Piranha solid state detector for this investigation was thus based on its prevalence and availability in most medical physics departments. Being a solid-state detector (rather than a spherical ionisation chamber as recommended by IEC

(2014)[1]), it is acknowledged that the Piranha is not an ideal choice of QA dosimeter to use for the purposes of lead equivalence testing. However, in terms of energy response, the Piranha has a kQ factor close to unity for beam qualities between 2.5- and 6.5-mm Al, i.e., being one of the better routinely available clinical detectors to use for this purpose[13]. The performance outcomes with this solid state detector and CBTK have demonstrated a high level of precision, thus our hope is to encourage other sites to implement lead equivalence testing QA programs with equipment that is readily available to enable such tests to become more routine and prevalent.

Conclusion

Acceptance testing of newly purchased radiation protection garments offers an assessment of (i) the integrity of material within the radiation protection garment via fluoroscopic screening, and importantly (ii) the attenuating capabilities of the radiation protection garment via lead equivalence testing, independent to that carried out by the manufacturer. Although our broad beam setup was designed to simultaneously comply with multiple standards, the measurement accuracy achieved throughout the study is a testament to the design and setup using the CBTK. The differential between labelled and measured lead equivalence was on average 3% for both pure lead samples and N-Pb samples, with an uncertainty of less than 7%. These performance tests demonstrated the robustness of the CBTK through the consistency of measurements achieved and minimization of setup errors. Within the limit of uncertainties, at 102 kVp the use of Cu or Al as added filtration has marginal effect on the measured lead equivalence outcomes of pure lead or N-Pb samples.

Declarations

Conflicts of interest/Competing interests

Authors have no conflicts of interest to disclose.

Author Contributions

All authors contributed to the study conception and design. Material preparation, design and development of the custom-built testing kit was performed by Robert Parin. Data collection and analysis was performed by Lesley Maddox under the direction of Benjamin Khoo. The first draft of the manuscript was written by Lesley Maddox and Benjamin Khoo has commented on previous versions and approved the final manuscript.

Funding

No funding was received for conducting this study.

References

1. IEC 61331-1:2014 (2014) Protective devices against diagnostic medical X-radiation – Part 1: Determination of attenuation properties of materials, International Electrotechnical Commission, Version 2.0
2. Australian/New Zealand Standard: AS/NZS 4543.1:1999 (IEC 61331-1:1994) (1999) Protective devices against diagnostic medical X-radiation – Part 1: Determination of attenuation properties of materials
3. IEC 61331-1:1994 (1994) Protective devices against diagnostic medical X-radiation – Part 1: Determination of attenuation properties of materials, International Electrotechnical Commission, Version 1.0
4. ARPANSA (2015) Aprons for protection against X-rays, Australian Government – Australian Radiation Protection and Nuclear Safety Agency, Fact Sheet 28 https://www.arpansa.gov.au/understanding-radiation/radiation-

sources/more-radiation-sources/aprons-protection-against-x-rays. Accessed 2 December 2020

5. M J Yaffe, G E Mawdsley, M Lilley, R Servant, G Reh (1991) Composite materials for x-ray protection, Health Physics 60(5):661-664
6. Australian/New Zealand Standard: AS/NZS 4543.3:2000 (2000) Protective devices against diagnostic medical X-radiation – Part 3: Protective clothing and protective devices for gonads
7. K Jones, L Wagner (2013) One the (f)utility of measuring the lead equivalence of protective garments, Journal of Med Phys, 40 (6)
8. Radiological Council of Western Australia (2015), Diagnostic X-ray Equipment Compliance Testing – Major Digital Radiographic Equipment, Department of Health – The Government of Western Australia under the Radiation Safety Act 1975
9. National Institute of Standards and Technology, X-ray Form Factor, Attenuation, and Scattering Tables https://physics.nist.gov/PhysRefData/FFast/html/form.html. Accessed 1 February 2021
10. J T Bushberg, J A Seibert, E M Leidholdt, J M Boone (2002) The Essential Physics of Medical Imaging, 2nd Edition, Lippincott Williams & Wilkins, USA
11. J Laban Understanding Lead Aprons - Setting the Standards, RADsafe https://radsafemedical.com/resources/understanding-lead-aprons/setting-the-standards/. Accessed 5 May 2022
12. H Eder, W Panzer, H Schöfer (2005) Is the lead-equivalent suited for rating protection properties of lead-free radiation protective clothing? Rofo, Fortschr.Röntgenstr. 177, 399-404
13. D R Dance et al (2014), Diagnostic Radiology Physics – A Handbook for Teachers and Students, International Atomic Energy Agency (IAEA), Vienna

Figures

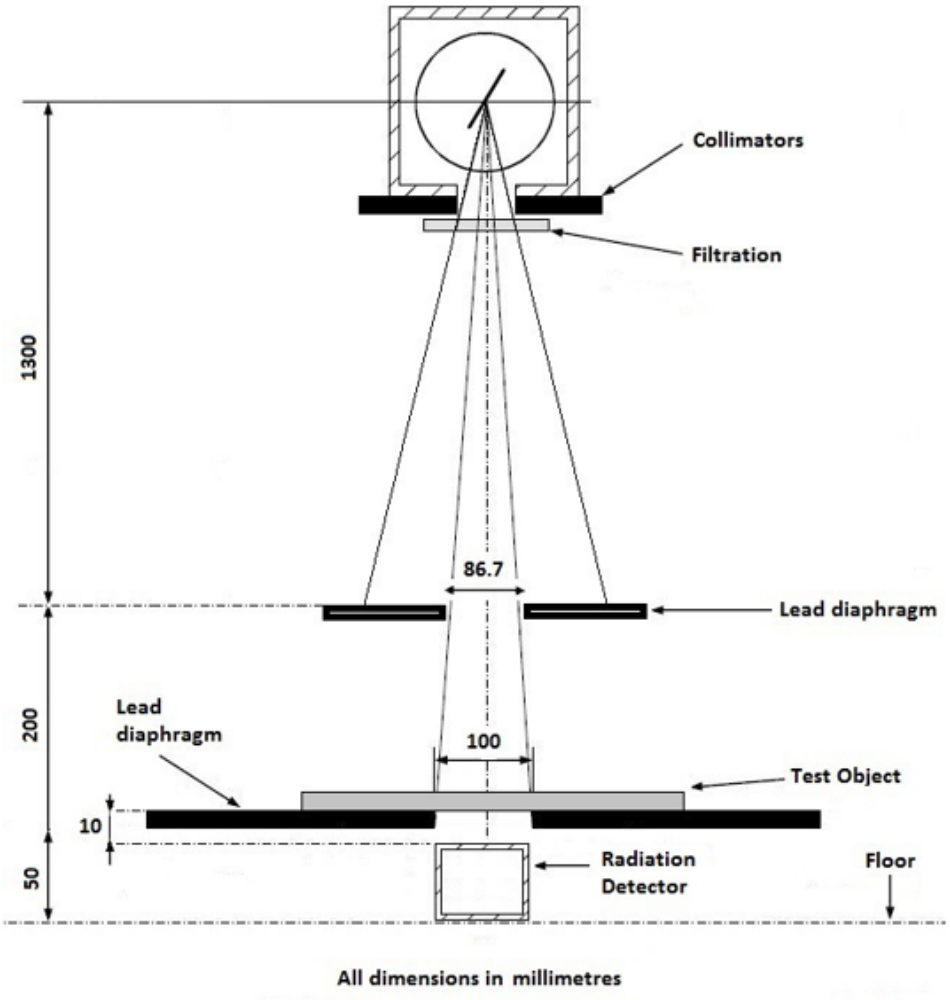

Figure 1

Amalgamated version of the broad beam geometry from IEC[1,3], AS/NZS[2] and ARPANSA[4]. The choice of filtration will determine which IEC standard the test is compliant with. This diagram was modified from the broad beam geometry published in IEC (2014) [1] with quantitative distances amended to the original copy based on our interpretation of the standard and is not to be confused with the original version of the diagram.

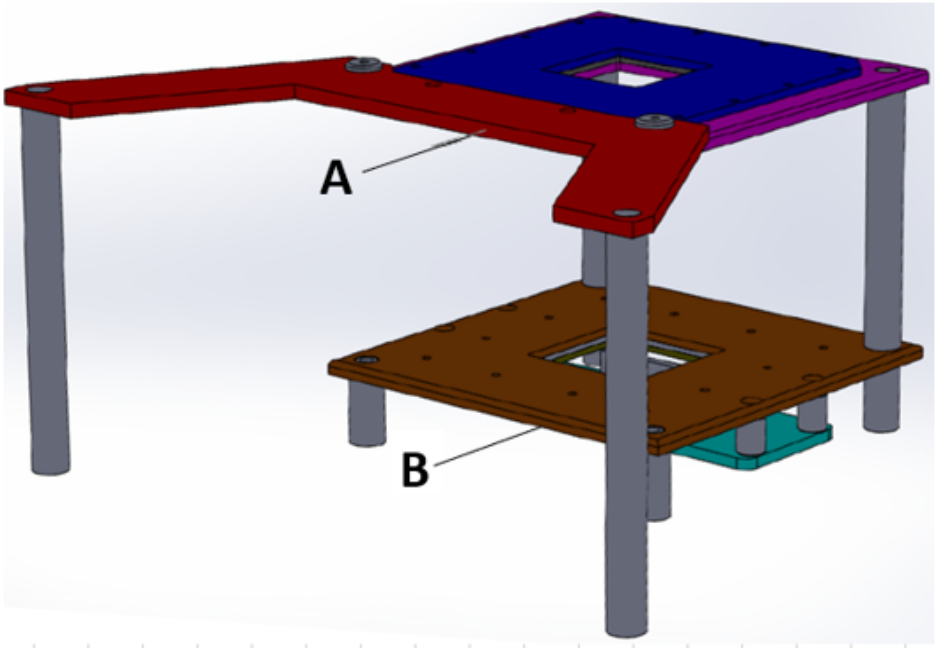

Figure 2

The custom-built lead equivalence testing kit (CBTK) contains two beam shaping lead diaphragms (A and B) which serve to collimate the x-ray field as defined by the broad beam conditions. Legs suspend the whole apparatus off the floor and the lower diaphragm (B) provides a platform on which the samples can be placed. A cradle was built underneath diaphragm B elevates the radiation detector above the floor and maintains it at a consistent distance as close to the sample as possible.

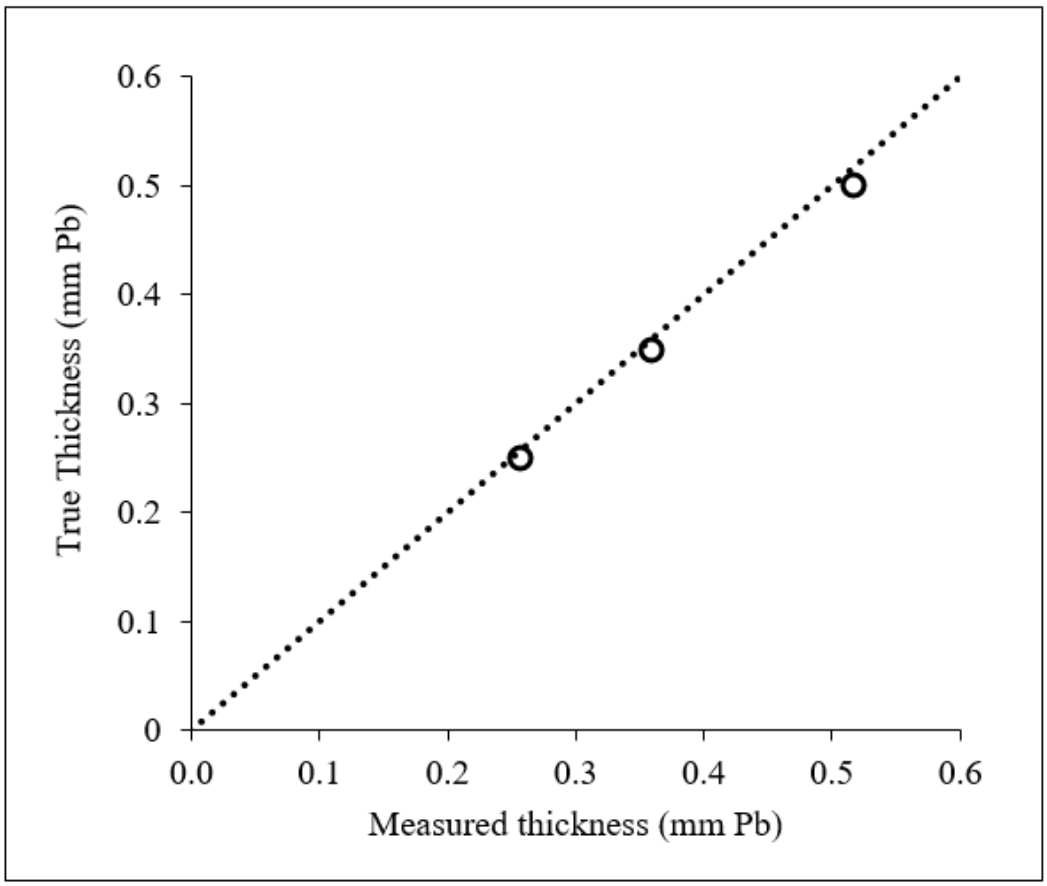

Figure 3

Verification samples of 0.25, 0.35 and 0.50 mm Pb (97%) (using 0.25mmCu filtration) were tested for their lead equivalence and calibration corrected (circular datapoints). Plotted against the line of unity (dotted line), the measured thickness shows strong agreement to the true thickness of these samples.

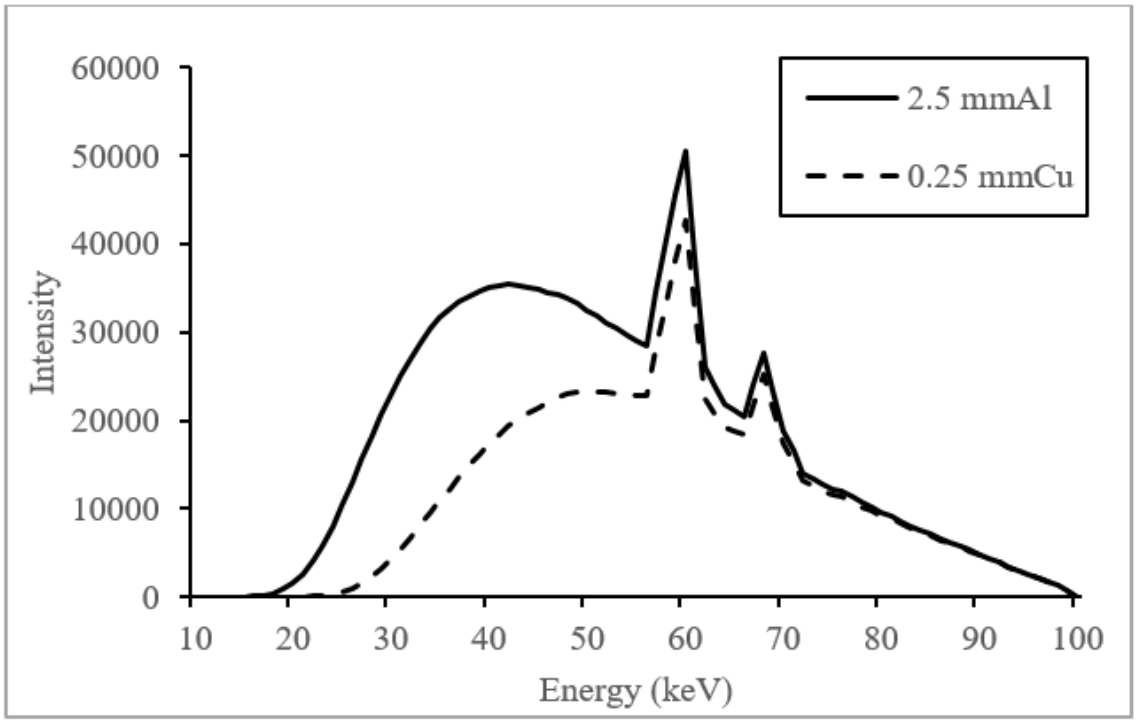

Figure 4

A comparison between the filtered bremsstrahlung spectra through 0.25 mmCu and 2.5 mmAl.

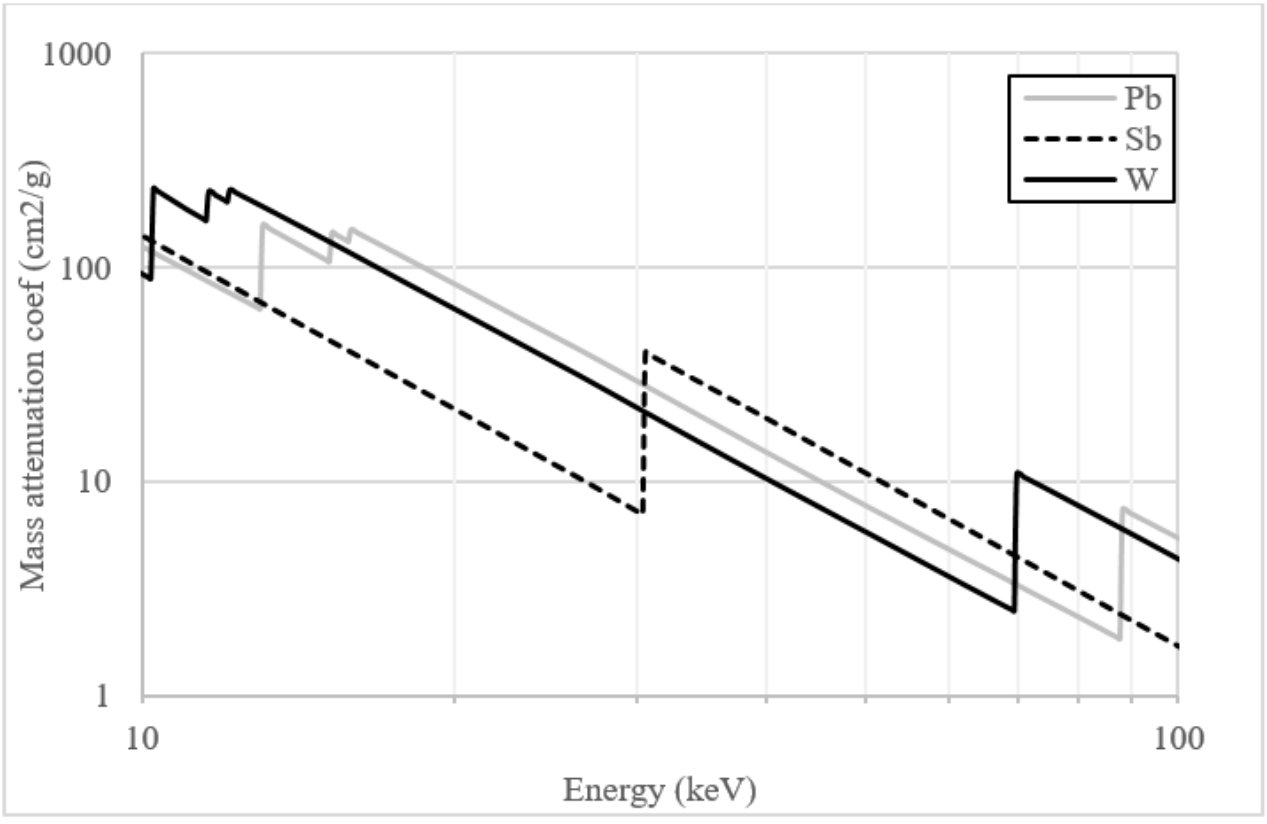

Figure 5

K- and L-edge curves for lead (Pb), antimony (Sb) and tungsten (W). [Data sourced from NIST[9]].